

Comprehensive Reinvestigation of Carbodiimide Guanylation: HCl-Initiated Access to Tri- and Tetrasubstituted Guanidines

Lukáš Vlk, Karel Pauk, Maksim A. Samsonov, Zdenka Růžicková, Tomáš Chlupatý,* and Aleš Růžicka*

Cite This: *ACS Omega* 2026, 11, 24075–24085

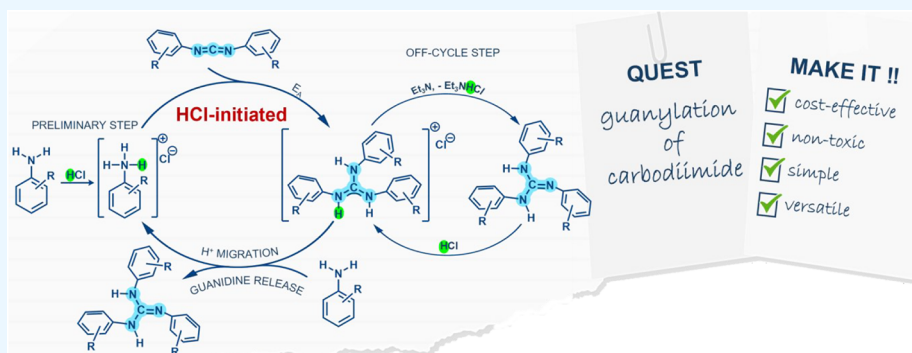
Read Online

ACCESS |

Metrics & More

Article Recommendations

Supporting Information



ABSTRACT: Guanidines are well-known π -electron-conjugated organic bases used widely in synthesis as well as in industry, with more than 150 years of history. Hence, a plethora of synthetic approaches leading to the formation of the central N_3C motif has been published, from conventional methods to more sophisticated catalysts. Despite this, some substrates are still not easily obtainable, and the reported procedures lack simplicity and universality. Here, procedures yielding guanidines from carbodiimides and various amines are provided. Thermally conducted reactions of aliphatic amines and carbodiimides led to guanidines, but efforts to extend this method to anilines failed, even with basic or some acidic catalysts. However, when HCl was added to the reaction media at >80 °C, guanidine products were successfully prepared. Thorough mechanistic investigations revealed the complexity of the guanylation, including several proton transfers, the unconventional switch of the reaction mechanism to electrophilic addition, and the regeneration of the catalytically active species. The process was optimized and applicable to a series of various substrates with the use of substoichiometric or even catalytic amounts of HCl. Guanidine structures, the guanylation mechanism, and prototropic tautomerism of aryl-substituted guanidines in solution were investigated by sXRD, NMR spectroscopy, and DFT calculations. An optimized, easy, cheap, and high-yield metal-free procedure catalyzed by HCl was described.

INTRODUCTION

Guanidines are considered organic superbases due to the $n-\pi$ conjugation of the central N_3C part and a push–pull effect,^{1,2} with the imino nitrogen being the most basic moiety of the molecule.² The spatial arrangement and characteristics of the N -atoms surrounding the central carbon atom of the N_3C unit provide significant configurability and tunability, which are influenced by steric and electronic effects. In their neutral form, they are useful in organic synthesis or as (non)nucleophilic catalysts,^{1,3–9} as Barton's bases resistant to alkylation,^{4,5,10} and have been associated with a range of biological activities, which is linked to the presence of the guanidine moiety in many natural products.^{11,12} Also, guanidines have been utilized in the pharmaceutical¹³ and food and petrochemical industries.¹ On the other hand, guanidinium cations show exceptional stability due to effective charge delocalization (Y -aromaticity),¹⁴ the robustness of the cation, and the ability to form hydrogen bonds, and they have been used as building blocks in the design of many organic and semiorganic materials.¹⁵ Neutral and anionic forms

have been widely used as ligands for the stabilization of various metals/elements in different oxidation states.^{16–20}

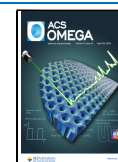
Two general routes exist for guanidine synthesis. Classical methods, using the nucleophilicity/basicity of amines, employ guanylation agents, such as thioureas, isothioureas, aminoiminomethanesulfonic acids, cyanamides, and carbodiimides, and often require activated substrates,^{21,22} increased temperature, toxic or difficult-to-achieve catalysts that are nontolerant to functional groups, and/or offer low yields (Figure 1).^{16,21–24} Thiophilic metal salts like Hg(II), Cu(II), or Sc(III) acetates or chlorides are the most common.^{25,26} In the case of carbodiimides, the guanylation of aliphatic amines is feasible

Received: November 26, 2025

Revised: March 27, 2026

Accepted: April 6, 2026

Published: April 16, 2026



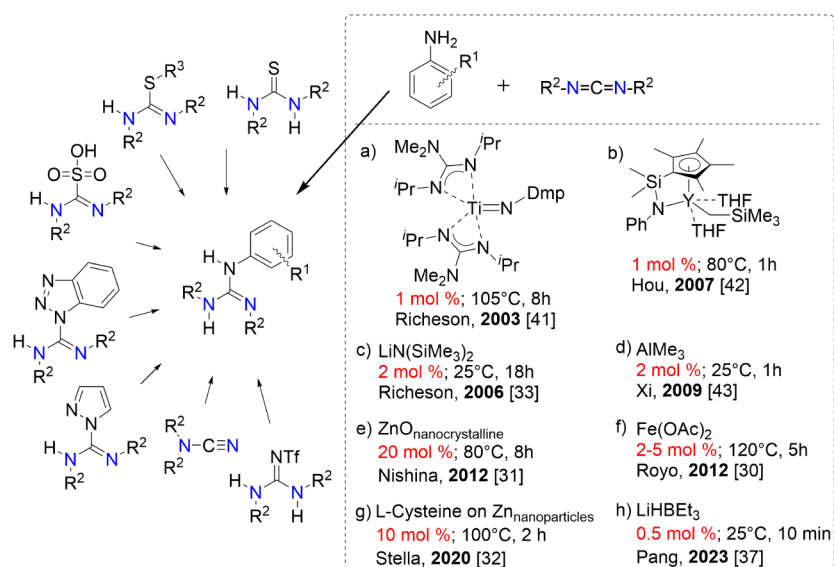


Figure 1. Overview of classical approaches for the guanylation reactions of amines. The guanylation protocol of carbodiimide and aromatic amines using selected catalysts is highlighted in the box. Appropriate references are given in square brackets.

when only thermally conducted, but this guanylation protocol with aromatic amines is insufficient unless initiated or activated (Figure 1) by a usually stoichiometric amount of an obscure/toxic initiator.

In contrast, the modern route using the catalyzed carbodiimide–amine system offers accessibility to plenty of substituted carbodiimides and overcomes the classical method's obstacles (Figure 1—highlighted box). These methodologies can sometimes bring challenges in terms of price, air instability, availability of the catalysts, together with respect for environmental aspects. To illustrate, guanylation of aniline with CDI^{Pr} under mild conditions with low loading of half-sandwich complexes of Y, Lu, Er (and others) as catalysts achieved high to almost quantitative conversion.²⁷ The reaction of similar substrates catalyzed by the less active dinuclear Ti(IV) amido complex required longer heating.²⁸ If a high-spin NHC-containing Fe(II) imido complex is used at 5 mol % for the guanylation of aliphatic carbodiimides with a series of anilines, conversions surpass 80% at room temperature after 15 h.²⁹ Some metal oxo-species, such as Fe(II) acetate,³⁰ ZnO nanoparticles,³¹ or Zn–S–cysteine nanoparticles,³² exhibited lower efficiency. In the field of main group element complexes (Li, Mg, Al, B), similar behavior to transition metal-based catalysts was observed.^{33–37} Guanylations of diisopropylcarbodiimide with selected functionalized anilines, such as 2-bromoaniline or *p*-anisidine, initiated by tris(pentafluorophenyl)borane,³⁸ also revealed good effectiveness for activated substrates. SnCl₄ was used to catalyze the annulation of 2-aminobenzonitrile and carbodiimides recently.³⁹ During the completion of this work, the guanylation of aliphatic amines, anilines, (sulfon)amides, ureas, and carbamates by guanidinium salt (HATU), leading to pentasubstituted guanidines, was described.^{40–43}

As illustrated in Figure 1, there is a plethora of excellent catalytic systems for the guanylation of carbodiimide described in the literature that are able to achieve high conversion at mild conditions or using relatively cheap, commercially available chemicals (for example, Me₃Al). However, none of these systems reaches all the characteristics of an all-round/universal catalyst, and the protocols suffer from drawbacks such as the use of a (sometimes toxic) metal or limitations in scope. The most

effective catalysts are usually unavailable and sensitive to moisture, while the air-stable species require much higher loading due to lower efficiency (ZnO nanoparticles). This work has the ambition to fulfill the requirements of a simple synthesis of structurally and electronically flexible guanidines while making the synthetic protocol cheap, green, unified, substrate-universal, and atom-efficient.

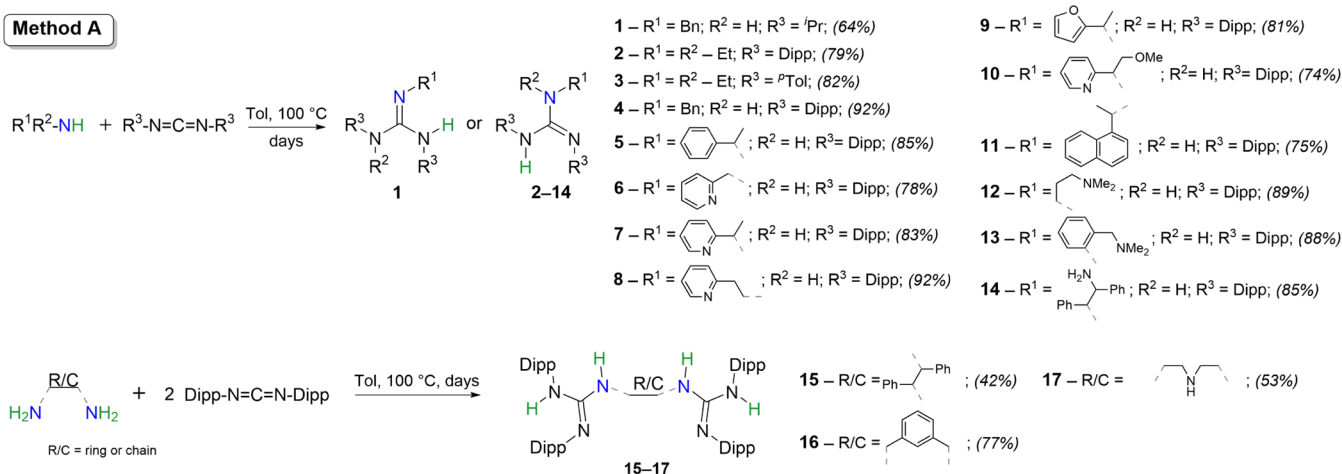
RESULTS AND DISCUSSION

Guanidines 1–17 (Scheme 1) were prepared by a classical guanylation approach²¹ via noncatalyzed thermal nucleophilic addition of an amine to the polarized cumulated NCN double bonds of the carbodiimide moiety in commercial-grade toluene at 100 °C for day(s) (dependent on the nature of the amine and monitored by ¹H NMR spectroscopy)—**Method A** (for a list of compounds, see Figure S1). Various aliphatic amines and diamines (including also (hetero)aromatic moieties) and *N,N'*-disubstituted carbodiimides (ⁱPr, ^tol, Dipp) gave appropriate guanidines of analytical purity after recrystallization/distillation in high to excellent yields. In the case of guanidine 13, an aromatic amine was used as the starting material, which can be classified more as an aliphatic amine in this guanylation protocol because of the activation of the NH₂ group through an intramolecular hydrogen bond to the NMe₂ group. This subsequently results in enhanced nucleophilicity and increased basicity. Attempts to prepare the monoguanidine analogue of 16 (1:1 ratio product) ended in an equimolar mixture of mono- and bis(guanidine) due to a competing reaction on both amino groups.

To broaden the scope to anilines, a protocol effective for aliphatic amines failed. No guanidine products were detected by NMR spectroscopy, even after prolonged heating of the mixture of CDIs and anilines. Similarly, acid or base catalysis (NaOH or CH₃COOH) or the introduction of donor functional groups to the aniline did not yield successful results. Surprisingly, the addition of a few drops of aqueous HCl (the same result was obtained with an anhydrous HCl/CPME solution under Ar) at 100 °C in toluene caused the formation of guanidine (21) along with the corresponding guanidinium. No conversion was detected by NMR spectroscopy below 80 °C. The reaction

Scheme 1. Synthesis of Guanidines 1–17 via Noncatalyzed Thermal Guanylation of Carbodiimides (Dipp = 2,6-Diisopropylphenyl).^a

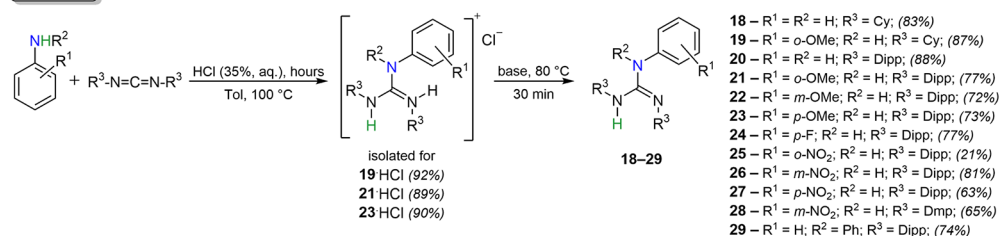
Method A



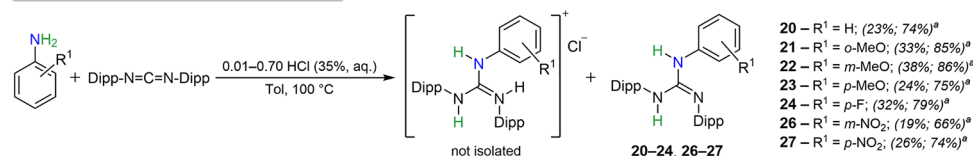
^aIsolated yields of target guanidines are given in parentheses.

Scheme 2. Synthesis of Guanidines 18–29 (and Guanidiniums 19·HCl, 21·HCl, and 23·HCl) via the HCl-Initiated Guanylation of Carbodiimidesⁱ

Method B



Method C - substoichiometric amount of HCl



ⁱBase—Et₃N (‘BuOK for 19·HCl). Isolated yields of target guanidines (Method B) and NMR yields after 2 days using 50 mol % of HCl (Method C) are given in parentheses, where the first number^a corresponds to free guanidine and the second to the sum of free guanidine and its guanidinium

mixture was further treated with a base (Et₃N or ‘BuOK), and only guanidine was obtained, which inspired further investigation of various substrates using a defined amount of HCl.

First trials conducted for reactions of *o*- or *p*-anisidine with CDI^{Dipp} and a stoichiometric amount of HCl (Scheme 2—Method B) yielded the conjugated acids of 21 and 23 (denoted as 21·HCl and 23·HCl) quantitatively after 1 h. However, these reactions ended in the guanidinium form, which requires an additional neutralization step and thus may, in some cases, be complex. This approach was extended to other primary aromatic amines (*o*-/*m*-/*p*-MeO, *p*-F, *o*-/*m*-/*p*-NO₂) and substituted CDIs (Cy, Dipp, Dmp), resulting in guanidines 18–28 (Scheme 2 and Figure S2 in ESI) after 12 h of heating in toluene, followed by *in situ* neutralization by Et₃N (or ‘BuOK in THF for isolated 19·HCl). During the review process of this article, the most challenging system was identified by one of the reviewers. As a proof-of-concept evaluation, one tetrasubstituted tetraarylguanidine 29 was successfully prepared under an identical protocol. To prevent the easy oxidation of the aliphatic CDI under acidic

conditions, the guanylations to 18 and 19 were performed under an inert argon atmosphere. Unexpectedly, during the synthesis of 25, which originated from an aromatic CDI and *o*-nitroaniline, a significant amount of urea (as well as its protonated form) was observed, even when the reaction was conducted under argon. A negligible increase in the yield of 25 (21% to 28%) was achieved when the amount of HCl was reduced to 50 mol %.

During the guanylation of the aniline series, it became evident that HCl plays a pivotal role in the reaction mechanism, indicating the greater complexity of the process. To elucidate this mechanism further, the impact of varying substoichiometric/catalytic amounts of HCl on the guanylation of aromatic substrates was investigated (Scheme 2—Method C). Specifically, the synthesis of 21 (also present as 21·HCl) from *o*-anisidine and CDI^{Dipp} was examined using 1–70 mol % of HCl over time (Figures 2 and S9 in ESI). The yields were quantified as a sum of guanidine (21) and its guanidinium (21·HCl), or only 21, over the duration of the reaction, while the amount of

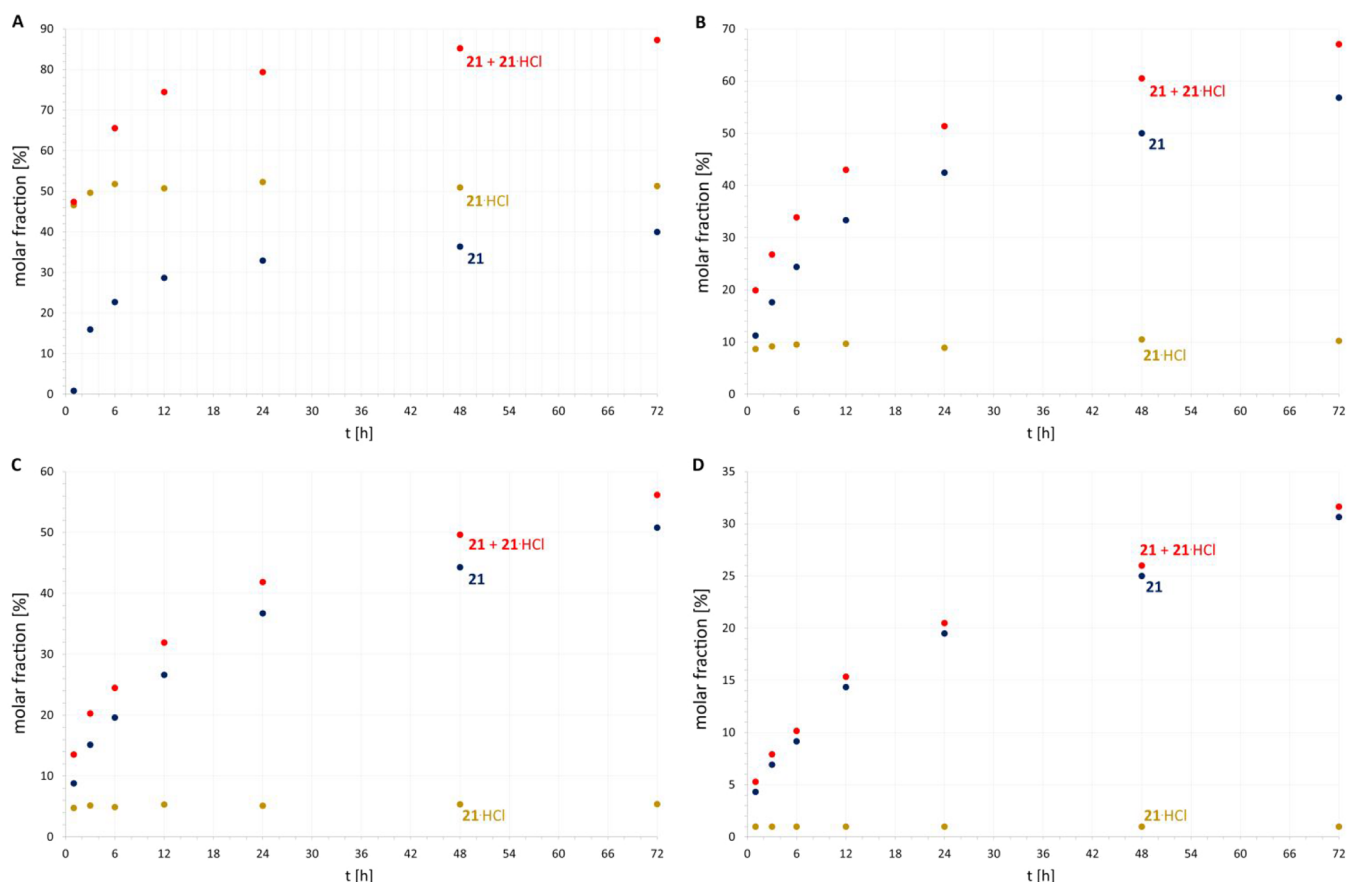


Figure 2. NMR yields of guanylation reactions of CDI^{DIPP} by *o*-anisidine to **21** (blue dots), **21·HCl** (gold dots), or to the cumulative yield of **21** and **21·HCl** (red dots) using: **A)** 50 mol % of HCl; **B)** 10 mol % of HCl; **C)** 5 mol % of HCl; and **D)** 1 mol % of HCl after 3 days.

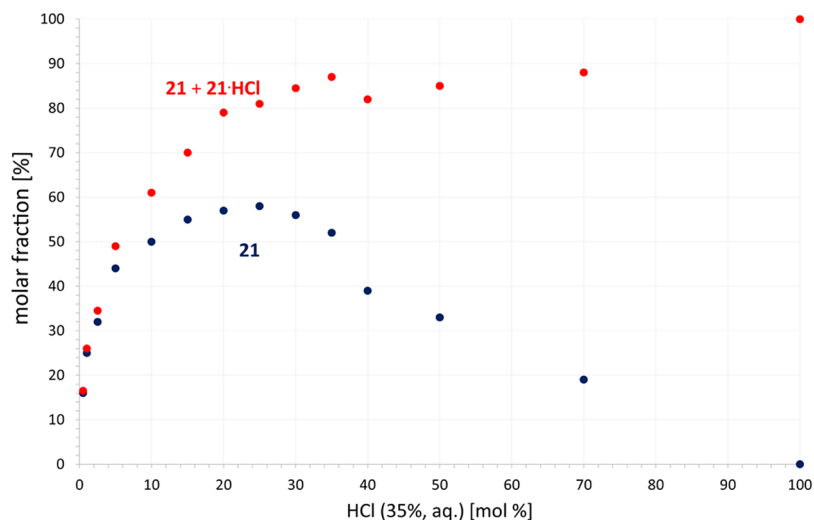


Figure 3. Optimization of the HCl amount for the preparation of **21** (blue dots) or the sum of **21** and **21·HCl** (red dots) after 2 days.

guanidinium remains constant throughout the whole process and is equal to the amount of HCl used (Figure 2). It should be considered that prolonged heating can lead to the oxidation/degradation of substrates. The findings from the guanylation protocol suggest that using a larger amount of HCl leads to an almost complete reaction (**21·HCl** predominates in the mixtures) within 3 days. Moreover, when a small initiator concentration (under 10 mol %) is used, there is still a significant increase in the yield of **21** due to a lower concentration of **21·**

HCl. For instance, the reaction with 50 mol % of HCl produced 29% of **21** after 1 day, with the yield rising to only 40% by day 7. In contrast, when only 1 mol % of HCl was utilized, the yield increased from 19% to 44%. To complete this hypothesis, the catalytic efficiency was screened using 1–100 mol % of HCl loading, plotted as yield against catalyst concentration (Figure 3), showing maximum yield of **21** at 25 mol % of HCl.

Expanding the portfolio of that method, it was applied to other anilines with the addition of 10 and 50 mol % HCl

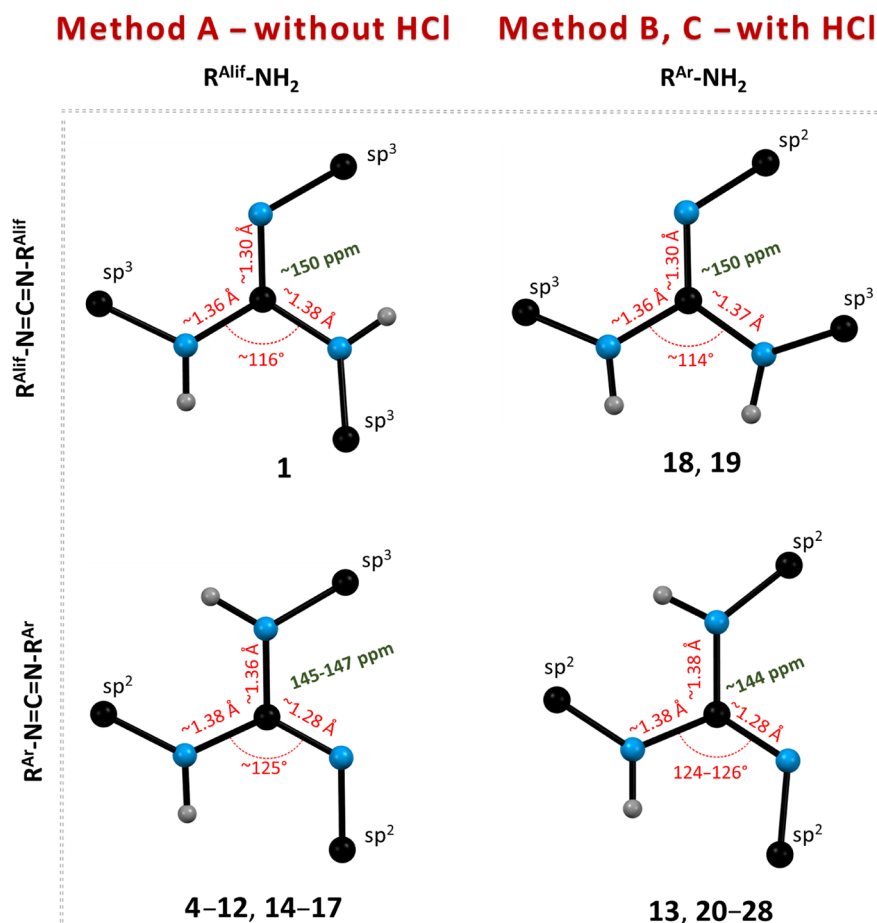


Figure 4. Illustration of selected structural parameters of guanidines, encompassing all four typological combinations. Blue spheres represent N atoms, black for C atoms, and gray for H-atoms. The ^{13}C NMR chemical shifts of Ar_q^{Gua} are shown in green.

(Scheme 2—Method C), covering various functional groups in different aromatic ring positions, including aniline (20—Figure S8), anisidines (22–23—Figures S10–S11), *p*-fluoroaniline (24—Figure S11), and nitroanilines (26–27—Figures S12–S13).

The overall basicity of the respective aniline is a contribution of mesomeric effects, and induction effects are the determining factors on which the reaction course depends. For the catalytic guanylation, the essential prerequisite is anilines' high proton affinity to form a conjugated pair with HCl (anilinium). This is evident in the case of the two *meta*-substituted anilines (better-performing *m*-OCH₃ going to 22 vs *m*-NO₂ going to 26), also compared to unsubstituted aniline for the formation of 20 (see SI, Table S2). Another comparison can be drawn between *o*-OCH₃ (21) and *m*-OCH₃ (22), where the yields to 21 are *ca* 20% higher. This was more pronounced in comparative experiments with 10% HCl, where yields were 15% for 26, 31% for 22, and 42% for 21 after 1 day (Table S2).

All isolated guanidines 1–29, covering all four typological combinations of starting aliphatic (R^{Alif})/aromatic (R^{Ar}) (Figure 4) amines and carbodiimides, and guanidiniums 19·HCl, 21·HCl, and 23·HCl were completely characterized by multi-nuclear NMR, MALDI-MS, scXRD (except for 3, 9, 11, and 16; Figures S16–S43 in ESI) techniques, and elemental analysis (20–29, 21·HCl and 23·HCl) (for an overview of the structural characterization methods used, see Figures S1–S2 in ESI). The most significant phenomena used for monitoring the course of the reaction were the hydrogen shift(s) from the starting amino

group to nitrogen atom(s) originating from the CDI moiety (change of ^1H NMR spectral pattern or chemical shift) and the related downfield shift of the central carbon atom (Ar_q^{Gua}) in ^{13}C NMR spectra. In nearly solvent-independent ^1H NMR spectra, the NH hydrogen atoms are chemically nonequivalent (except for 1, 18, and 19). For 13 and 25, one NH (originating from aniline) is downfield-shifted because of an intramolecular H-bond. The deshielding of Ar_q^{Gua} was observed in ^{13}C spectra for all prepared guanidines, with typical values of ~ 150 ppm for tri-/tetrasubstituted di-/trialkylguanidines 1–3, 18, 19, and 29 (measured at 240 K in Tol-*d*₈), while for trisubstituted di-/triarylguanidines 4–17 and 20–28, the values range between 144–147 ppm. To complete the structural description, the C–N distances of the N_3C unit show partial π -electron delocalization for all guanidines ($\text{C}^{\text{Gua}}\text{—NH}$: 1.36–1.39 Å and $\text{C}^{\text{Gua}}\text{—N}$: ~ 1.30 Å) (Figure 4), with slight differences for tetraarylguanidine 29 (Figure S43).

In the NMR spectra of “aromatic” guanidines 20–27 and 29, originating from the anilines and aromatic CDI^{Dipp}, a second minor set of signals with similar chemical shift values was observed. This phenomenon was more pronounced in THF-*d*₆ (for 29, observed in Tol-*d*₈ at 240 and 273 K—Figures S70–S71) solution and was further investigated for an extreme example of 26 by VT-NMR spectroscopy (Figures S4–S7 in ESI) and DFT calculations (Figure 6). Eighteen mol % of the minor form was detected at room temperature in THF-*d*₆, contrary to 9 mol % in C₆D₆, while only negligible temperature dependency was observed by VT-NMR measurements in both

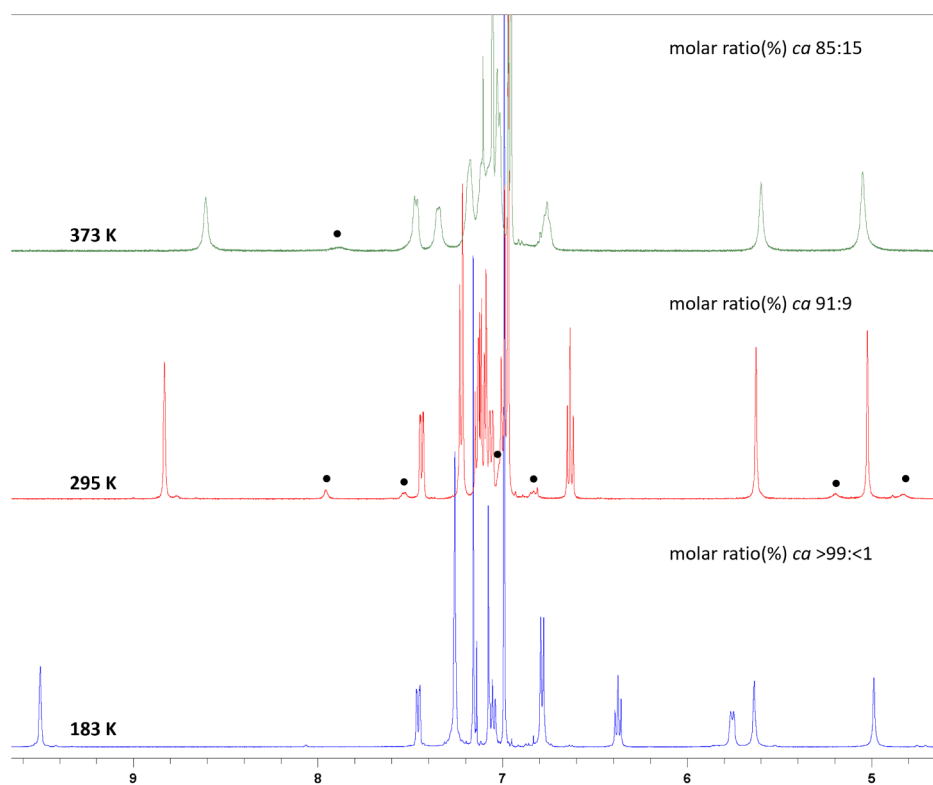


Figure 5. Detail of VT ^1H NMR spectra of **26** in Tol- d_8 at 183–373 K. Signals of the minor tautomer are marked with black dots.

solvents (see Figures S5–S7). However, a significant change of the relative populations of both species was observed in Tol- d_8 in the range of 183–373 K (Figures 5 and S7 in ESI).

This was initially attributed to prototropic guanidine tautomerism/isomerism. The structures of four reliable conformers/isomers, constructed from both *ab initio* or *scXRD*/optimized geometries, were prepared. For these species, the NMR shielding constants for ^{13}C nuclei were calculated by the GIAO method (B3LYP/6–311+g(d,p)/D3/CPCM(THF)).⁴⁴ The most probable isomers/conformers of **26** were selected based on the direct comparison of the structures, Gibbs' free energies (Figure 6),⁴⁵ and calculated (Table S1, Figure S3) vs measured ^{13}C NMR parameters in THF- d_8 solution.

Two of the four relevant isomers, specifically the pair of rotamers **26A** and **26A'** (Figure 6), exhibit a minimal energy difference of just 1 kcal·mol⁻¹ in THF (virtually identical in C₆H₆). Moreover, the rotation barrier from **26A** to **26A'** is only 3.7 kcal·mol⁻¹. These isomers are thus indistinguishable in solution by NMR spectroscopy, and their weighted chemical shifts represent the signals of the major isomer of **26**. According to the Boltzmann distribution at room temperature, their respective contributions to the chemical shift values are 15.4% for **26A** and 84.6% for **26A'** (Table S1, Figure S3). For isomer **26B**, analysis of the correlation between the measured signals in the ^{13}C NMR spectra and the calculated chemical shieldings indicates that it exists as a minor form in solution NMR (Table S1, Figure S3). In contrast, isomer **26C**, despite being energetically similar, was not detected in either the solution or the solid state.

To provide a deeper understanding of the guanylation mechanism, we conducted a detailed investigation of the *o*-anisidine-CDI^{Dipp}-HCl system using NMR and DFT techniques at the B3LYP/cc-pVTZ level of theory.⁴⁵ It clearly showed that the process begins with the immediate protonation of the aniline

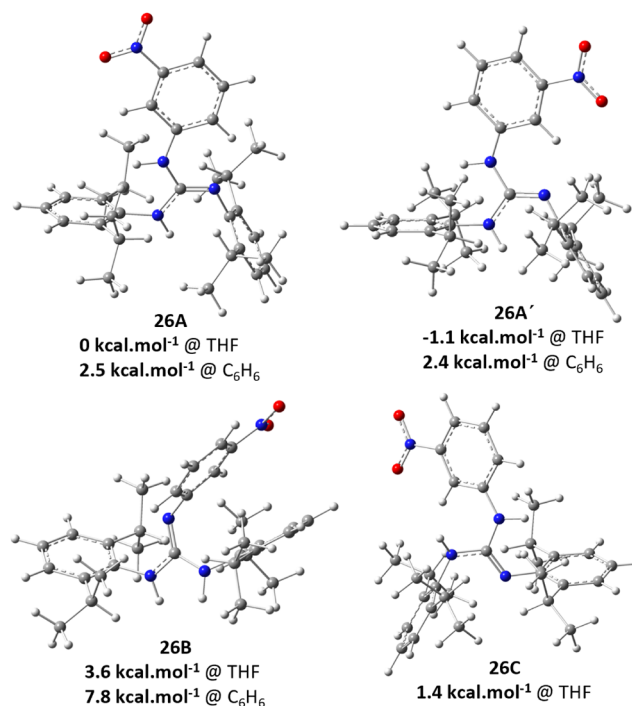


Figure 6. Optimized structures of possible tautomers/isomers of **26**, along with relative Gibbs' free energies.

to INT-1 (Figure 7; rather than a less basic CDI^{Dipp}). This was also evidenced by the fast proton transfer from individually prepared H⁺CDI^{Dipp} and *o*-anisidine.

The thermodynamically lowest **21**·HCl species (−20.31 kcal·mol⁻¹) is produced through several consecutive steps (Figure 8 and Figure S14 in ESI), virtually connected by several H-bond

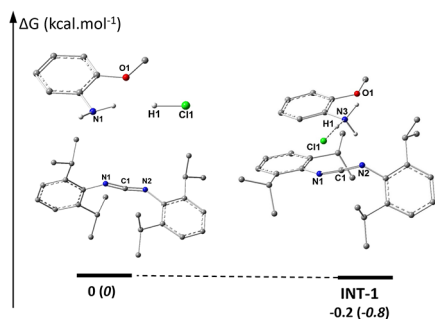


Figure 7. DFT-estimated Gibbs free energy profile ($\text{kcal}\cdot\text{mol}^{-1}$) for the calculated interaction between *o*-anisidine (values for *p*-anisidine are given in parentheses), CDI^{DIPP} , and the HCl molecule.

interactions. From INT-1, H1 from the amino group connects the aniline to the CDI of INT-2, thus bringing the N3 and C1 atoms into proximity. The energetically limiting step is TS-2 ($7.75 \text{ kcal}\cdot\text{mol}^{-1}$), where the N3–C1 bond is formed, followed by an intramolecular proton transfer of H2 (via INT-1 to TS-3). The proposed slow migration of the proton from 21·HCl to the next starting *o*-anisidine molecule (TS-4, $\Delta\Delta G$: $18.67 \text{ kcal}\cdot\text{mol}^{-1}$) allows the initiation of a new catalytic cycle (blue lines in profile). The guanidine 21 is released and accumulates over time, which is compensated for by the fast generation of another new 21·HCl. An alternative pathway, which is more thermodynamically favored, is the neutralization of 21·HCl by Et_3N addition—TS-4' (the red trace in Figure 4). To explore the influence of a sterically less demanding substrate of the same basicity, the same calculations were performed for *p*-anisidine to provide 23 (Figure 8 in parentheses), with negligible energy changes. When virtually replacing the proton within the mechanism for a metal ion, each individual reaction step would be similar. As expected, calculations of all four model systems, covering combinations of CDI-amine (aliphatic or

aromatic, Figure S15) showed thermodynamically favorable catalytic processes in the series of aliphatic amines. Based on these findings, additional guanylation experiments, mimicking a substoichiometric amount of acid catalyst, were successfully initiated by 50 mol % *o*-anisidinium hydrochloride or guanidinium 21·HCl (Scheme S1 in ESI). To be honest, there are decades-old papers reporting a few examples of ammonium salts and their interactions with carbodiimide (amine and carbodiimide in an acidic environment), but the results were misunderstood and useful details overlooked.^{46–53} Taking these reports into account, a stoichiometric reaction of *o*-anisidinium and 21 in toluene was performed, yielding exclusively 21·HCl and *o*-anisidine after 1 h, even at room temperature (Scheme S1 in ESI).

CONCLUSIONS

There is no comprehensive guanylation approach covering a wide array of substrates with respect to functional groups, while maintaining low economic and accessibility requirements. It is reasonable to assert that the literature describes numerous catalytic carbodiimide guanylation systems that exhibit enhanced conversion values and reduced reaction times; however, these systems are often constrained by limitations related to the steric accessibility or reactivity of substrates, as well as the use of toxic, sensitive, or difficult-to-obtain catalysts. In contrast, this study presents a cost-effective, nontoxic, and universally applicable alternative for the synthesis of tri- and tetrasubstituted guanidines, employing HCl as an initiator. Concretely, the suggested guanylation mechanism (to 21) was supported by extended model experiments and theoretical calculations. The rate-determining step, connected to the highest computed activation barrier for TS-4 (release of 21, $\Delta\Delta G = 18.67 \text{ kcal}\cdot\text{mol}^{-1}$), corresponds to the proton transfer from the earlier formed guanidinium to an adjacent molecule of aniline. The reaction time can be drastically shortened by

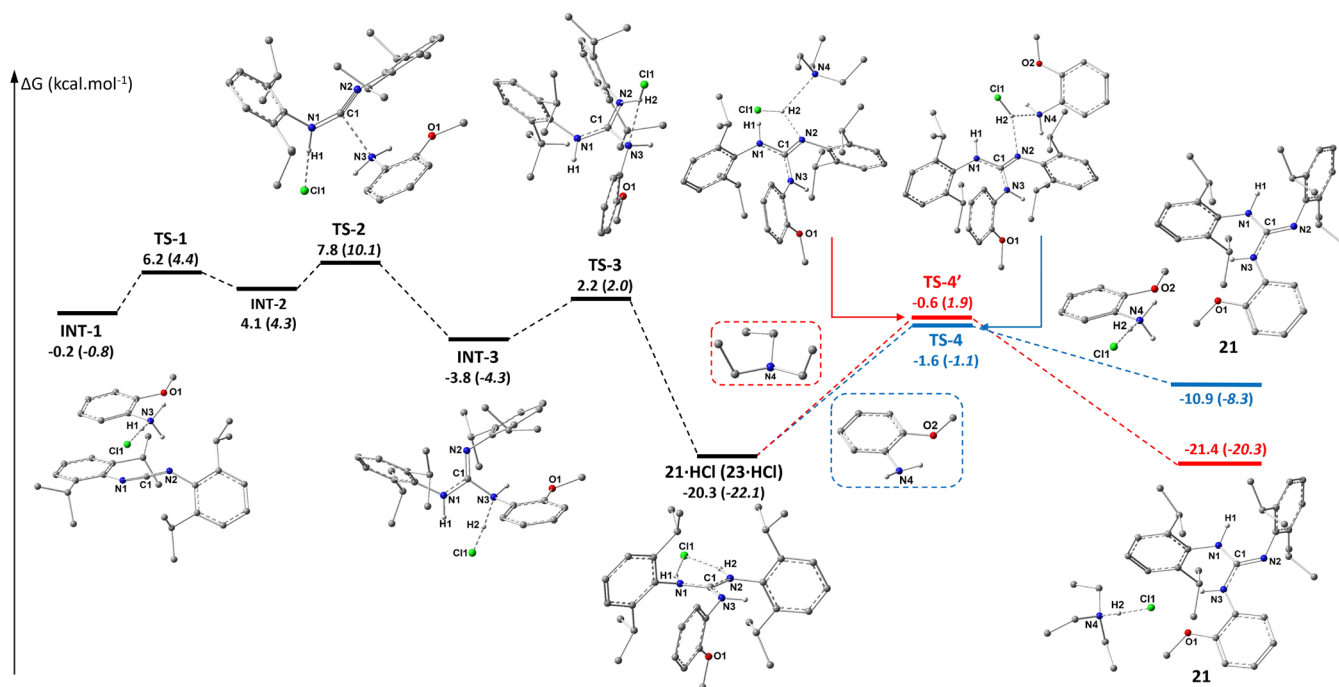


Figure 8. DFT-estimated Gibbs free energy profile ($\text{kcal}\cdot\text{mol}^{-1}$) for 21 (23 in italics in parentheses). The preliminary step to INT-1 (see Figure 7 above), and structures describing TS-1 and INT-2 are omitted for clarity. Full energy profile is available in Figure S14 in the ESI.

employing a higher amount of HCl, followed by the addition of a stronger base with subsequent workup.

MATERIALS AND METHODS

All solvents and chemical reagents were purchased from commercial sources and used without further purification. Some synthetic procedures were performed using standard Schlenk techniques under an inert argon atmosphere (99.999%) (the inert gas was passed through the oxygen/moisture trap Supelco before entering the vacuum/inert line), and solvents were dried with the help of the solvent purification system PureSolv MD 7 supplied by Innovative Technology, Inc., degassed, and then stored under an argon atmosphere over a potassium or sodium mirror, if needed. Single crystals suitable for X-ray analysis were obtained from the corresponding saturated solutions of products in organic solvent(s) cooled to 7 or -30 °C or by slow evaporation at room temperature. Deuterated solvents for NMR spectroscopy, if needed, were distilled, degassed, and stored over a K or Na mirror under an argon atmosphere.

Elemental analysis (C, H, N, Cl) was performed on an automatic microanalyser Flash 2000 Organic Elemental Analyzer. Mass spectrometry with high resolution was determined by the “dried droplet” method using a MALDI LTQ Orbitrap XL mass spectrometer (Thermo Fisher Scientific) equipped with a nitrogen UV laser (337 nm, 60 Hz). Spectra were measured in positive ion mode and in regular mass extent with a resolution of 100,000 at a mass-to-charge ratio (m/z) of 400, with 2,5-dihydrobenzoic acid (DHB) used as the matrix. Mass spectrum of **29** was performed on Vanquish HPLC/ISQ system from Thermo Scientific equipped with a quaternary pump (VC-P20-A), split sampler (VC-A12-A), column compartment (VC-C10-A), diode array detector (VC-D11-A), and mass spectrometer (ISQ ICMS Family).

NMR spectra were recorded from solutions of appropriate compounds in deuterated solvent(s) on a Bruker Avance 500 spectrometer (equipped with a Z-gradient 5 mm Prodigy cryoprobe) at frequencies for ^1H (500.13 MHz), $^{13}\text{C}\{^1\text{H}\}$ (125.76 MHz), and ^{15}N (50.66 MHz) or on a Bruker UltraShield 400 spectrometer at frequencies for ^1H (400.13 MHz) and $^{13}\text{C}\{^1\text{H}\}$ (100.58 MHz) at 295 K, or in some cases, at various temperatures. Solutions were obtained by dissolving approximately 40 mg of each compound in 0.6 mL of deuterated solvents. Values of ^1H chemical shifts were calibrated to residual signals of benzene ($\delta(^1\text{H}) = 7.16$), THF ($\delta(^1\text{H}) = 1.73$), toluene ($\delta(^1\text{H}) = 2.09$), or DMSO ($\delta(^1\text{H}) = 2.50$). Values of ^{13}C chemical shifts were calibrated to signals of THF ($\delta(^{13}\text{C}) = 67.6$), benzene ($\delta(^{13}\text{C}) = 128.4$), toluene ($\delta(^{13}\text{C}) = 20.4$), or DMSO ($\delta(^{13}\text{C}) = 20.4$), and ^{15}N to external nitromethane ($\delta(^{15}\text{N}) = 0.0$). All ^{13}C NMR spectra were measured using a standard proton-decoupled experiment, and CH and CH_3 vs C and CH_2 were differentiated with the help of the APT method.⁵⁴ Determination of signals of chemically nonequivalent protons, carbon, and nitrogen atoms in the NMR spectra was supported by $^1\text{H}, ^1\text{H}-\text{COSY}$, $^1\text{H}, ^1\text{H}-\text{NOESY}$, $^1\text{H}, ^{13}\text{C}-\text{HSQC}$ or/and $^1\text{H}, ^{13}\text{C}-\text{HMBC}$ techniques.

General Methods for Guanylation Reactions (1–29)

Method A: Guanylation without HCl (1–17). To a round-bottom flask equipped with a condenser, one equivalent of colorless N,N' -diisopropylcarbodiimide, 1,3-di-*p*-tolylcarbodiimide, or N,N' -bis(2,6-diisopropylphenyl)carbodiimide with one (or half) equivalent of the appropriate aliphatic (except **13**) amine/diamine was dissolved in toluene. The reaction mixture was refluxed for several days, depending on the type of amine (2–19 days). After that, the toluene was evaporated under vacuum, and the crude products were purified by recrystallization from organic solvent(s) or by distillation (for **1**).

Method B: Guanylation with a Stoichiometric Amount of HCl (18–29, 19-HCl, 21-HCl, and 23-HCl). To a round-bottom flask equipped with a condenser, one equivalent of colorless N,N' -dicyclohexylcarbodiimide, N,N' -bis(2,6-dimethylphenyl)carbodiimide, or N,N' -bis(2,6-diisopropylphenyl)carbodiimide with one equivalent of an appropriate aromatic amine was dissolved in toluene, followed by the addition of the same equivalent of HCl solution. The reaction mixture became heterogeneous and was heated to 100 °C overnight, with

subsequent cooling to room temperature. Appropriate crude guanidinium chlorides were formed.

In the case of 19-HCl, 21-HCl, and 23-HCl, crude products were additionally isolated by filtration and purified by washing/recrystallization from organic solvent. However, for **25**, all solvents from the reaction mixture were evaporated, the crude product (mainly guanidinium) was washed by a large portion of Et_2O and suspended in hexane.

Then, 1.1 equiv of Et_3N was added to the mixture (all protonated forms were transformed to their neutral species), which led to the gradual precipitation of a white solid, $\text{Et}_3\text{N}-\text{HCl}$, for 30 min at 80 °C (except 19-HCl— $t\text{-BuOK}$ in THF). After that, the prepared guanidines **19–28** were filtered off, toluene was evaporated under vacuum, and the crude products were purified by recrystallization from organic solvent(s). Details of the complex purification process for **18** are described below.

Method C: Guanylation with a Substoichiometric Amount of HCl (20–24, 26–27). To a round-bottom flask equipped with a condenser, colorless N,N' -bis(2,6-diisopropylphenyl)carbodiimide (0.5 g, 1.38 mmol) with one equivalent of the appropriate aromatic amine was dissolved in toluene (30 mL), followed by the addition of a substoichiometric amount of HCl solution (35% aqueous solution, $\rho = 1.180 \text{ g}\cdot\text{cm}^{-3}$), which caused the immediate formation of a white precipitate (related to the amount of HCl). The reaction mixture was heated to 100 °C for a certain period, which depended on the degree of conversion monitored by the integration of ^1H NMR spectra in THF- d_6 of reaction mixture aliquots over the timeline.

In some cases, Et_3N (10% excess relative to HCl) was added to the mixture, which led to the gradual precipitation of a white solid, $\text{Et}_3\text{N}-\text{HCl}$, in 30 min at 80 °C. All protonated forms were transformed to their neutral species to confirm the amount of formed guanidines, as determined by NMR yield, without further isolation/purification.

Crystallography

Full sets of diffraction data for **2, 4–8, 10, 12–14, and 17** (see Tables S4–S13 and S15) were obtained at 150 K using an Oxford Cryostream low-temperature device on a Nonius KappaCCD diffractometer with MoK_α radiation ($\lambda = 0.71073 \text{ \AA}$), a graphite monochromator, and the ϕ and χ scan mode. Data reductions were performed with DENZO-SMN.⁵⁵ The absorption was corrected by the multiscan method—SADABS or by integration methods.⁵⁶ Structures were solved by direct methods (Sir92)⁵⁷ and refined by full-matrix least-squares based on F^2 (SHELXL97).⁵⁸

Full sets of diffraction data for **1, 15, 18–29, 19-HCl, 21-HCl, and 23-HCl** (see Tables S3, S14, and S16–S30) were collected at 150(2)K with a Bruker D8-Venture diffractometer equipped with Cu (Cu/K_α radiation; $\lambda = 1.54178 \text{ \AA}$) or Mo (Mo/K_α radiation; $\lambda = 0.71073 \text{ \AA}$) microfocus X-ray ($I\mu\text{S}$) sources. A photon CMOS detector and an Oxford Cryosystems cooling device were used for data collection.

The frames were integrated with the Bruker SAINT software package by using a narrow frame algorithm. Data were corrected for absorption effects using the multiscan method (SADABS). The obtained data were treated by XT-version 2014/5 and SHELXL-2017/1 software implemented in the APEX3 v2016.5–0 (Bruker AXS) system.⁵⁹

Hydrogen atoms were mostly localized on a difference Fourier map; however, to ensure uniformity in the treatment of the crystal, all hydrogen atoms were recalculated into idealized positions (riding model) and assigned temperature factors $\text{H}_{\text{iso}}(\text{H}) = 1.2 U_{\text{eq}}$ (pivot atom) or $1.5 U_{\text{eq}}$ (methyl). H atoms in methyl, methylene, moieties, and hydrogen atoms in aromatic rings were placed with C–H distances of 0.96, 0.97, and 0.93 Å, respectively. Hydrogen atoms of N–H groups were refined freely or with fixed distances of 0.92 Å. Disordered parts of isopropyl and coordinated THF molecules in **1** were treated by standard methods.

Crystallographic data for structural analysis have been deposited with the Cambridge Crystallographic Data Center, CCDC 2120564–2120577, 2120580–2120589, 2382648–2382649, 2442574, and 2524367 for **1–2, 4–8, 10, 12–15, 17–29, 19-HCl, 21-HCl, and 23-HCl**. Copies of this information may be obtained free of charge from The Director, CCDC, 12 Union Road, Cambridge CB2 1EY, UK (fax:

+44–1223–336033; e-mail: deposit@ccdc.cam.ac.uk or www: <http://www.ccdc.cam.ac.uk>).

DFT Calculations

All calculations were performed using the Gaussian 16 program.⁶⁰ Reaction energy profiles were computed at the B3LYP/cc-pVTZ,⁴⁵ level of theory, incorporating solvation effects through the polarizable continuum model (PCM)⁴⁴ for toluene. Additionally, dispersion corrections were applied using the D3 version of Grimme's dispersion method.⁶¹ Frequency analysis at the same level of theory confirmed that all computed structures correspond to minima on the potential energy surface, with transition states exhibiting a single imaginary frequency.

■ ASSOCIATED CONTENT

Data Availability Statement

Complete NMR spectra (DOI: <http://10.6084/m9.figshare.28816364>) of all prepared compounds.

Supporting Information

The Supporting Information is available free of charge at <https://pubs.acs.org/doi/10.1021/acsomega.5c12436>.

Synthetic procedures, explanation of structures, and tautomerism (DOCX)

(CIF)

(CIF)

(CIF)

Guanylation mechanism (XYZ)

Complete NMR spectra of all prepared compounds (PDF)

■ AUTHOR INFORMATION

Corresponding Authors

Tomáš Chlupatý – Department of General and Inorganic Chemistry, Faculty of Chemical Technology, University of Pardubice, Pardubice CZ-532 10, Czech Republic;

orcid.org/0000-0002-0883-5593;

Email: tomas.chlupaty@upce.cz

Aleš Růžička – Department of General and Inorganic Chemistry, Faculty of Chemical Technology, University of Pardubice, Pardubice CZ-532 10, Czech Republic;

orcid.org/0000-0001-8191-0273; Email: ales.ruzicka@upce.cz

Authors

Lukáš Vlk – Department of General and Inorganic Chemistry, Faculty of Chemical Technology, University of Pardubice, Pardubice CZ-532 10, Czech Republic

Karel Pauk – Institute of Organic Chemistry and Technology, Faculty of Chemical Technology, University of Pardubice, Pardubice CZ-532 10, Czech Republic

Maksim A. Samsonov – Department of General and Inorganic Chemistry, Faculty of Chemical Technology, University of Pardubice, Pardubice CZ-532 10, Czech Republic

Zdeňka Růžičková – Department of General and Inorganic Chemistry, Faculty of Chemical Technology, University of Pardubice, Pardubice CZ-532 10, Czech Republic

Complete contact information is available at:

<https://pubs.acs.org/doi/10.1021/acsomega.5c12436>

Author Contributions

The manuscript was written through the contributions of all authors. All authors have given approval to the final version of the manuscript. L.V.: synthesis, investigation, writing; K.P.:

characterization, analysis; M.A.S.: DFT; Z.R.: X-ray diffraction analysis; T.C.: investigation, writing, NMR spectroscopy, conceptualization; A.R.: conceptualization, supervision, X-ray diffraction analysis, writing.

Notes

The authors declare no competing financial interest.

■ ACKNOWLEDGMENTS

This work was supported by the Czech Science Foundation Grant No. 25-17434S. This work has been funded by a grant from the Programme Johannes Amos Comenius under the Ministry of Education, Youth and Sports of the Czech Republic [No. CZ.02.01.01/00/23_021/0008593]. M.Sc. Natalia Gira and M.Sc. Emilie Riemlová are thanked for their support with specific synthetic tasks.

■ REFERENCES

- (1) *Superbases for Organic Synthesis: Guanidines, Amidines, Phosphazenes and Related Organocatalysts*; Ishikawa, P. T., ed.; John Wiley & Sons, Ltd.: Chichester, 2009. DOI: .
- (2) Raczyńska, E. D.; Gal, J. F.; Maria, P. C. Enhanced Basicity of Push-Pull Nitrogen Bases in the Gas Phase. *Chem. Rev.* **2016**, *116* (22), 13454–13511.
- (3) Taylor, J. E.; Bull, S. D.; Williams, J. M. Amidines, isothioureas, and guanidines as nucleophilic catalysts. *Chem. Soc. Rev.* **2012**, *41* (6), 2109–2121.
- (4) Smedley, C. J.; Homer, J. A.; Gialelis, T. L.; Barrow, A. S.; Koelln, R. A.; Moses, J. E. Accelerated SuFEx Click Chemistry For Modular Synthesis. *Angew. Chem., Int. Ed.* **2022**, *61* (4), No. e202112375.
- (5) Muzyka, C.; Renson, S.; Grignard, B.; Detrembleur, C.; Monbaliu, J. M. Intensified Continuous Flow Process for the Scalable Production of Bio-Based Glycerol Carbonate. *Angew. Chem., Int. Ed.* **2024**, *63* (10), No. e202319060.
- (6) Mannisto, J. K.; Sahari, A.; Lagerblom, K.; Niemi, T.; Nieger, M.; Sztano, G.; Repo, T. One-Step Synthesis of 3,4-Disubstituted 2-Oxazolidinones by Base-Catalyzed CO₂ Fixation and Aza-Michael Addition. *Chem.–Eur. J.* **2019**, *25* (44), 10284–10289.
- (7) Mannisto, J. K.; Pavlovic, L.; Heikkinen, J.; Tiainen, T.; Sahari, A.; Maier, N. M.; Rissanen, K.; Nieger, M.; Hopmann, K. H.; Repo, T. N-Heteroaryl Carbamates from Carbon Dioxide via Chemoselective Superbase Catalysis: Substrate Scope and Mechanistic Investigation. *ACS Catal.* **2023**, *13* (17), 11509–11521.
- (8) Morack, T.; Myers, T. E.; Karas, L. J.; Hardy, M. A.; Mercado, B. Q.; Sigman, M. S.; Miller, S. J. An Asymmetric Aromatic Finkelstein Reaction: A Platform for Remote Diarylmethane Desymmetrization. *J. Am. Chem. Soc.* **2023**, *145* (41), 22322–22328.
- (9) Chinn, A. J.; Kim, B.; Kwon, Y.; Miller, S. J. Enantioselective Intermolecular C–O Bond Formation in the Desymmetrization of Diarylmethines Employing a Guanidinylated Peptide-Based Catalyst. *J. Am. Chem. Soc.* **2017**, *139* (49), 18107–18114.
- (10) Barton, D.; Elliott, J.; Géro, S. Synthesis and properties of a series of sterically hindered guanidine bases. *J. Chem. Soc., Perkin Trans.* **1982**, *1*, 2085–2090.
- (11) Berlinck, R. G. S.; Bertonha, A. F.; Takaki, M.; Rodriguez, J. P. G. The chemistry and biology of guanidine natural products. *Nat. Prod. Rep.* **2017**, *34* (11), 1264–1301.
- (12) Somberg, N. H.; Sućec, I.; Medeiros-Silva, J.; Jo, H.; Beres, R.; Syed, A. M.; Doudna, J. A.; Hong, M. Oligomeric State and Drug Binding of the SARS-CoV-2 Envelope Protein Are Sensitive to the Ectodomain. *J. Am. Chem. Soc.* **2024**, *146* (35), 24537–24552.
- (13) von Itzstein, M. The war against influenza: discovery and development of sialidase inhibitors. *Nat. Rev. Drug Discovery* **2007**, *6*, 967–974.
- (14) Gund, P. Guanidine, trimethylenemethane, and “Y-delocalization.” Can acyclic compounds have “aromatic” stability? *J. Chem. Educ.* **1972**, *49*, 100–103.

- (15) Pei, T.; Zhou, L.; Zhang, Q.; Ma, D.; Bai, Y.; Yin, Q.; Xie, C. Studies on structure, NLO properties of a new organic NLO crystal: guanidinium 3,5-dihydroxybenzoate. *J. Mater. Sci.: Mater. Electron.* **2019**, *30*, 2994–3003.
- (16) Sengupta, D.; Gómez-Torres, A.; Fortier, S. Guanidinate, Amidinate, and Formamidinate Ligands. In *Comprehensive Coordination Chemistry III*, Constable, E. C.; Parkin, G.; Que, L., Jr, Eds.; Elsevier, 2021; pp. 366–405. DOI: .
- (17) Bailey, P. J.; Pace, S. The coordination chemistry of guanidines and guanidates. *Coord. Chem. Rev.* **2001**, *214* (1), 91–141.
- (18) Coles, M. P. Application of neutral amidines and guanidines in coordination chemistry. *Dalton Trans.* **2006**, No. 8, 985–1001.
- (19) Jones, C. Bulky guanidates for the stabilization of low oxidation state metallocycles. *Coord. Chem. Rev.* **2010**, *254* (11–12), 1273–1289.
- (20) Carrillo-Hermosilla, F.; Fernández-Galán, R.; Ramos, A.; Elorriaga, D. Guanidates as Alternative Ligands for Organometallic Complexes. *Molecules* **2022**, *27* (18), 5962–5992.
- (21) Alonso-Moreno, C.; Antinolo, A.; Carrillo-Hermosilla, F.; Otero, A. Guanidines: from classical approaches to efficient catalytic syntheses. *Chem. Soc. Rev.* **2014**, *43* (10), 3406–3425.
- (22) Takeuchi, K.; Nakayama, A.; Tanino, K.; Namba, K. Facile Guanidine Formation under Mild Acidic Conditions. *Synlett* **2016**, *27* (18), 2591–2596.
- (23) Maierhaba, J.; Bulunuer, Y.; Abudurehman, W. Catalyst and Additive-Free Direct Synthesis of N-Sulfonyl Guanidines. *Chin. J. Org. Chem.* **2024**, *44* (4), 1276–1283.
- (24) Zhang, W.-X.; Xu, L.; Xi, Z. Recent development of synthetic preparation methods for guanidines via transition metal catalysis. *Chem. Commun.* **2015**, *51* (2), 254–265.
- (25) Levallet, C.; Lerpiniere, J.; Ko, S. Y. The HgCl₂-promoted guanylation reaction: The scope and limitations. *Tetrahedron* **1997**, *53* (14), 5291–5304.
- (26) Tsubokura, K.; Iwata, T.; Taichi, M.; Kurbangalieva, A.; Fukase, K.; Nakao, Y.; Tanaka, K. Direct Guanylation of Amino Groups by Cyanamide in Water: Catalytic Generation and Activation of Unsubstituted Carbodiimide by Scandium(III) Triflate. *Synlett* **2014**, *25* (9), 1302–1306.
- (27) Xu, L.; Wang, Z.; Zhang, W.-X.; Xi, Z. Rare-Earth Metal Tris(trimethylsilylmethyl) Anionic Complexes Bearing One 1-Phenyl-2,3,4,5-tetrapropylcyclopentadienyl Ligand: Synthesis, Structural Characterization, and Application. *Inorg. Chem.* **2012**, *51* (21), 11941–11948.
- (28) Banerjee, I.; Sagar, S.; Lorber, C.; Panda, T. K. Catalytic addition reactions of amines, thiols, and diphenyl-phosphine oxides to heterocumulenes using a bridging Sulfonylimido titanium(IV) complex. *Z. Anorg. Allgem. Chem.* **2022**, *648* (18), No. e202200188.
- (29) Gao, Y.; Carta, V.; Pink, M.; Smith, J. M. Catalytic Carbodiimide Guanylation by a Nucleophilic, High Spin Iron(II) Imido Complex. *J. Am. Chem. Soc.* **2021**, *143* (14), 5324–5329.
- (30) Pottabathula, S.; Royo, B. First iron-catalyzed guanylation of amines: a simple and highly efficient protocol to guanidines. *Tetrahedron Lett.* **2012**, *53* (38), 5156–5158.
- (31) Kantam, M. L.; Priyadarshini, S.; Joseph, P. J. A.; Srinivas, P.; Vinu, A.; Klabunde, K. J.; Nishina, Y. Catalytic guanylation of aliphatic, aromatic, heterocyclic primary and secondary amines using nanocrystalline zinc(II) oxide. *Tetrahedron* **2012**, *68* (29), 5730–5737.
- (32) Muthuvinothini, A.; Stella, S. L-Cysteine capped Zn nanoparticles catalyzed synthesis of guanidines. *Synth. Commun.* **2021**, *51*, 461–470.
- (33) Ong, T.-G.; O'Brien, J. S.; Korobkov, I.; Richeson, D. S. Facile and Atom-Efficient Amidolithium-Catalyzed C–C and C–N Formation for the Construction of Substituted Guanidines and Propiolamidines. *Organometallics* **2006**, *25* (20), 4728–4730.
- (34) Lachs, J. R.; Barrett, A. G. M.; Crimmin, M. R.; Kociok-Köhn, G.; Hill, M. S.; Mahon, M. F.; Procopiou, P. A. Heavier Group-2-Element Catalyzed Hydroamination of Carbodiimides. *Eur. J. Inorg. Chem.* **2008**, *26*, 4173–4179.
- (35) Karmakar, H.; Anga, S.; Panda, T. K.; Chandrasekhar, V. Aluminium alkyl complexes supported by imino-phosphoramidate ligand as precursors for catalytic guanylation reactions of carbodiimides. *RSC Adv.* **2022**, *12* (8), 4501–4509.
- (36) Nayak, D. K.; Sarkar, N.; Sampath, C. M.; Sahoo, R. K.; Nembenna, S. Organoaluminum Catalyzed Guanylation and Hydroboration Reactions of Carbodiimides. *Z. Anorg. Allgem. Chem.* **2022**, *648* (19), No. e202200116.
- (37) Du, Z.; Wen, X.; Pang, Z. Hydroamination of Carbodiimides Catalyzed by Lithium Triethylborohydride. *Synthesis* **2023**, *55*, 1079–1088.
- (38) Antiñolo, A.; Carrillo-Hermosilla, F.; Fernández-Galán, R.; Martínez-Ferrer, J.; Alonso-Moreno, C.; Bravo, I.; Moreno-Blázquez, S.; Salgado, M.; Villaseñor, E.; Albaladejo, J. Tris(pentafluorophenyl)-borane as an efficient catalyst in the guanylation reaction of amines. *Dalton Trans.* **2016**, *45* (26), 10717–10729.
- (39) Porashar, B.; Choudhury, C.; Saikia, A. K. Synthesis of 2,4-Diaminoquinazolines and 2-Amino-4-iminoquinazolines via Substrate-Controlled Annulation of 2-Aminobenzonitriles and Carbodiimides. *ChemistrySelect* **2025**, *10*, No. e202405899.
- (40) Aho, J. A. S.; Mannisto, J. K.; Mattila, S. P. M.; Hallamaa, M.; Deska, J. Guanidium Unmasked: Repurposing Common Amide Coupling Reagents for the Synthesis of Pentasubstituted Guanidine Bases. *J. Org. Chem.* **2025**, *90* (7), 2636–2643.
- (41) Ong, T. G.; Yap, G. P. A.; Richeson, D. S. Catalytic Construction and Reconstruction of Guanidines: Ti-Mediated Guanylation of Amines and Transamination of Guanidines. *J. Am. Chem. Soc.* **2003**, *125*, 8100–8101.
- (42) Zhang, W.-X.; Nishiura, M.; Hou, Z. Catalytic Addition of Amine N-H Bonds to Carbodiimides by Half-Sandwich Rare-Earth Metal Complexes: Efficient Synthesis of Substituted Guanidines through Amine Protonolysis of Rare-Earth Metal Guanidates. *Chem.–Eur. J.* **2007**, *13*, 4037–4051.
- (43) Zhang, W.-X.; Li, D.; Wang, Z.; Xi, Z. Alkyl Aluminum-Catalyzed Addition of Amines to Carbodiimides: A Highly Efficient Route to Substituted Guanidines. *Organometallics* **2009**, *28*, 882–887.
- (b) Becke, A. D. Density functional thermochemistry. III. The role of exact exchange. *J. Chem. Phys.* **1993**, *98* (7), 5648–5652.
- (44) Tomasi, J.; Mennucci, B.; Cammi, R. Quantum Mechanical Continuum Solvation Models. *Chem. Rev.* **2005**, *105*, 2999–3094.
- (45) Dunning, T. H. Gaussian basis sets for use in correlated molecular calculations. I. The atoms boron through neon and hydrogen. *J. Chem. Phys.* **1989**, *90* (2), 1007–1023.
- (46) Dorokhov, V. A.; Shagova, E. A.; Novikova, T. S.; Sheremetev, A. B.; Khmel'nitskii, L. I. Synthesis of guanidinofurazans from aminofurazans and carbodiimides. *Russ. Chem. Bull.* **1988**, *37*, 2128–2131.
- (47) Kurzer, F.; Sanderson, P. M. 38. Heterocyclic compounds from urea derivatives. Part V. Synthesis and cyclisation of N-o-hydroxyphenyl-N'-N''-diarylguanidines. *J. Chem. Soc.* **1963**, 240–245.
- (48) Kurzer, F.; Sanderson, P. M. 43. Heterocyclic compounds from urea derivatives. Part III. Synthesis and cyclisation of isothioureas derived from o-aminothiophenol and diarylcarbodi-imides. *J. Chem. Soc.* **1962**, 230–236.
- (49) Snedker, S. J. C. The mechanism of the formation of triphenylguanidine and phenylthiocarbimide from thiocarbanilide. *Trans. J. Chem. Technol. Biotechnol.* **1926**, *45* (41), T343–T354.
- (50) Weith, W. Ueber Carbodiphenylimid. *Ber. Dtsch. Chem. Ges.* **1874**, *7* (1), 10–16.
- (51) Weith, W. Ueber Tetraphenylguanidin und Diphenylcyanamid. *Ber. Dtsch. Chem. Ges.* **1874**, *7* (1), 843–853.
- (52) Huhn, A. Beiträge zur Kenntniss der aromatischen Carbodiimide. *Ber. Dtsch. Chem. Ges.* **1886**, *19* (2), 2404–2414.
- (53) Busch, M.; Blume, G.; Plungs, E. Zur Kenntnis der Carbodiimide. *J. Prakt. Chem.* **1909**, *79* (1), 513–546.
- (54) Patt, S. L.; Shoolery, J. N. Attached proton test for carbon-13 NMR. *J. Magn. Reson.* **1982**, *46*, 535–539.
- (55) Otwinowski, Z.; Minor, W. Processing of X-ray diffraction data collected in oscillation mode. *Methods Enzymol.* **1997**, *276*, 307–326.
- (56) *Crystallographic Computing* Ahmed, F. R.; Hall, S. R.; Huber, C. P., Eds.; International Booksellers and Publishers, 1970; pp. 255–270.

(57) Altomare, A.; Cascarano, G.; Giacovazzo, C.; Guagliardi, A. Early finding of preferred orientation: a new method. *J. Appl. Crystallogr.* **1994**, *27*, 1045–1050.

(58) Sheldrick, G. M. *SHELXL-97, A Program for Crystal Structure Refinement*; University of Göttingen: Göttingen, 2008.

(59) Sheldrick, G. M. Crystal structure refinement with SHELXL. *Acta Cryst. C* **2015**, *71*, 3–8.

(60) Frisch, M. J.; Trucks, G. W.; Schlegel, H. B.; Scuseria, G. E.; Robb, M. A.; Cheeseman, J. R.; Scalmani, G.; Barone, V.; Petersson, G. A.; Nakatsuji, H., et al. *Gaussian 16, Revision C.0 1*; Gaussian, Inc.: Wallingford CT, 2016.

(61) Grimme, S.; Antony, J.; Ehrlich, S.; Krieg, H. A consistent and accurate ab initio parametrization of density functional dispersion correction (DFT-D) for the 94 elements H-Pu. *J. Chem. Phys.* **2010**, *132*, 154104.



CAS INSIGHTS™

EXPLORE THE INNOVATIONS SHAPING TOMORROW

Discover the latest scientific research and trends with CAS Insights. Subscribe for email updates on new articles, reports, and webinars at the intersection of science and innovation.

Subscribe today

CAS
A Division of the
American Chemical Society